ACS SyntheticBiology

pubs.acs.org/synthbio Review

Transcription-Factor-based Biosensor Engineering for Applications in Synthetic Biology

Nana Ding, Shenghu Zhou,* and Yu Deng*

Cite This: https://doi.org/10.1021/acssynbio.0c00252 Read Online

ACCESS | Metrics & More | Article Recommendations

ABSTRACT: Transcription-factor-based biosensors (TFBs) are often used for metabolite detection, adaptive evolution, and metabolic flux control. However, designing TFBs with superior performance for applications in synthetic biology remains challenging. Specifically, natural TFBs often do not meet real-time detection requirements owing to their slow response times and inappropriate dynamic ranges, detection ranges, sensitivity, and selectivity. Furthermore, designing and optimizing complex dynamic regulation networks is time-consuming and labor-intensive. This Review highlights TFB-based applications and recent engineering strategies ranging from traditional trial-and-error approaches to novel computer-model-based rational design approaches. The limitations of the applications and these engineering strategies are additionally reviewed.

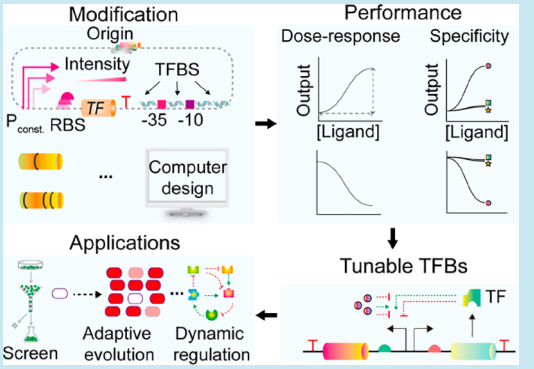

KEYWORDS: *high-throughput screening, adaptive evolution, dynamic regulation, genetic circuits, dose−response*

During compound production in microbial cell factories, real-time monitoring of metabolite concentrations is critical for the dynamic regulation of metabolic networks.[1] Therefore, biosensors that sense metabolites and regulate gene expression are increasingly attractive design goals.[2] Existing biosensors include nucleic-acid- and protein-based biosensors. Aptamers have often been used as building blocks for designing small-molecule nucleic-acid-based biosensors. Transcription-factor-based biosensors (TFBs) and riboswitches are the two most commonly used biosensors that can convert the signals of specific metabolite concentrations into a readout of the expression states of target genes.[3,4] In the signal response process, the allosteric effects of a regulator should be closely related to inducer concentration rather than irrelevant genetic contexts. The three-dimensional structures of riboswitches and aptamer-based biosensors are highly influenced by the surrounding conditions because the correct DNA or RNA conformation requires a suitable pH and ionic strength.[5,6] Furthermore, accurately predicting or detecting three-dimensional conformations of riboswitches and aptamers is difficult because their flexible structures hinder the formation of crystal structures with target metabolites. Compared with nucleic-acid-based biosensors, TFBs have substantial advantages in that their robustness enhances their performance under different production conditions.

TFBs are commonly used in quantitative metabolite determination,[7,8] high-throughput screening,[9] adaptive evolution,[10] and dynamic metabolic engineering applications[11−13] according to the different output signals. Their detectable fluorescence is often used as the output signal in quantitative metabolite determination and high-throughput screening.[8,14] Likewise, cell growth rates and metabolic pathway expression levels are often used as output signals in adaptive evolution and dynamic metabolic engineering applications,[15−17] respectively. However, constructed TFBs are often restricted by slow response times[5,18−20] as well as inappropriate dynamic ranges, detection ranges, sensitivity, and selectivity. These aspects result in unreliable output and delays in the signal response process, thus limiting the applications of TFBs in metabolic engineering and synthetic biology. Therefore, there is an urgent need to develop high-performance tunable TFBs to overcome the above challenges.

The key performance factors affecting TFB applications include (1) specificity, that is, the relative difference between an increase in output signal upon binding of a target ligand and the output signal upon binding to other potential ligands of interest;[21] (2) sensitivity, that is, the Hill coefficient of the fitted dose−response curve, describing the changes in speed of the output signal when the ligand concentration transitions from low to high;[21,22] (3) dynamic range, that is, the fold

Received: May 9, 2020

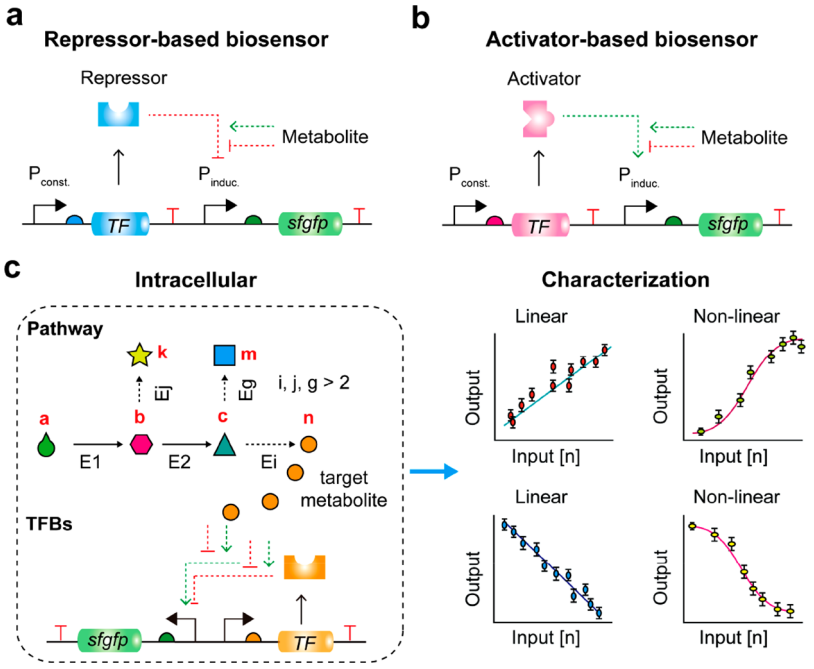

Figure 1. Responsive mechanisms of TFBs and applications in metabolite determination. (a) Repressor-based biosensor. A TF suppresses target gene expression in the presence or absence of the target metabolite. (b) Activator-based biosensor. A TF activates target gene expression in the presence or absence of the target metabolite. Red blunt-ended dashed arrows denote repression, and green dashed arrows indicate activation. $P_{const.}$ and $P_{induc.}$ represent the constitutive and inducible promoters, respectively. *sfgfp* is the superfolder GFP gene.[46] (c) Real-time monitoring of changes in the target metabolite concentration. Biosensors based on transcriptional activators or repressors can linearly or nonlinearly respond to target metabolite concentrations within the detection range. Ei represents the pathway enzymes. The substrate, intermediates, and final metabolites are marked a; b and c; and k, m, and n, respectively.

Table 1. Overview of Biosensor-based Measurements of Metabolite Concentrations

TFB	inducer	source	host	detection range	correlation
TetR[42]	aTc	*E. coli*	*E. coli*	4−50 ng/mL	nonlinear R^2 = 0.9987
LuxR[42]	$3OC_6HSL$	*V. fischeri*	*E. coli*	1.6−25000 nM	nonlinear R^2 = 0.9944
ArsR[42]	$NaAsO_2$	*E. coli*	*E. coli*	0.125−32 μM	nonlinear R^2 = 0.9964
FdeR[50]	naringenin	*H. seropedicae*	*S. cerevisiae*	0.094−0.184 mM	linear R^2 = 0.96
TbuT[51]	isoprene	*R. pickettii* PKO1	*E. coli*	0.05−2 mM	nonlinear
VanR[52]	vanillate	*C. crescentus*	*E. coli*	0.05−0.2 mM	linear R^2 = 0.68
PuuR[48]	putrescine	*E. coli*	*E. coli*	0.048−18.049 mg/g DW	linear R^2 = 0.95
FadR[53]	oleic acid	*E. coli*	*E. coli*	0.0001−1 mM	nonlinear
AcuR[54]	acrylate	*R. sphaeroides*	*E. coli*	0.016−10 mM	nonlinear
AraC[54]	arabinose	*E. coli*	*E. coli*	0−40 mM	nonlinear
CdaR[54]	glucarate	*E. coli*	*E. coli*	0−40 mM	nonlinear
MphR[54]	erythromycin	*E. coli*	*E. coli*	0−1400 μM	nonlinear
TtgR[54]	naringenin	*P. putida*	*E. coli*	110−9000 μM	nonlinear
ChnR/Pb[55]	butyrolactam	*Acinetobacter* sp. strain NCIMB9871	*E. coli*	1−100 mM	nonlinear
	valerolactam			1−50 mM	
	caprolactam			1−50 mM	
MphR[56]	erythromycin A (ErA)	*E. coli*	*E. coli*	0.1−10 μM	nonlinear
War1p[47]	C_6 fatty acids	*S. cerevisiae*	*S. cerevisiae*	0.01−2 mM	linear R^2 = 0.98
	C_7 fatty acids			0.01−1.5 mM	linear R^2 = 0.99
	C_8 fatty acids			0.01−0.75 mM	linear R^2 = 0.99
SRTF1[20]	progesterone	bacteria	*E. coli*	1−10000 nM	nonlinear
PuuR[48]	putrescine	*E. coli*	*E. coli*	50−608.6 mg/L	nonlinear R^2 = 0.96
TyrR[57]	tyrosine	*E. coli*	*E. coli*	5−100 mM	linear R^2 = 0.9771
	phenylalanine			5−100 mM	linear R^2 = 0.9964

change in gene expression in the presence *versus* the absence of an inducer;[23] (4) detection range, that is, the range between the lower and upper limits of measured inducer values;[24,25] and (5) response time, that is, the time when the signal reaches half the highest output signal after induction.[26] Inappropriate expression levels of transcription factors (TFs) and reporters not only lead to low TFB performances but also result in a metabolic burden on cells. Therefore, researchers have focused primarily on optimizing the expression levels of the TF and reporter by engineering regulatory elements, such as

https://doi.org/10.1021/acssynbio.0c00252
ACS Synth. Biol. XXXX, XXX, XXX−XXX

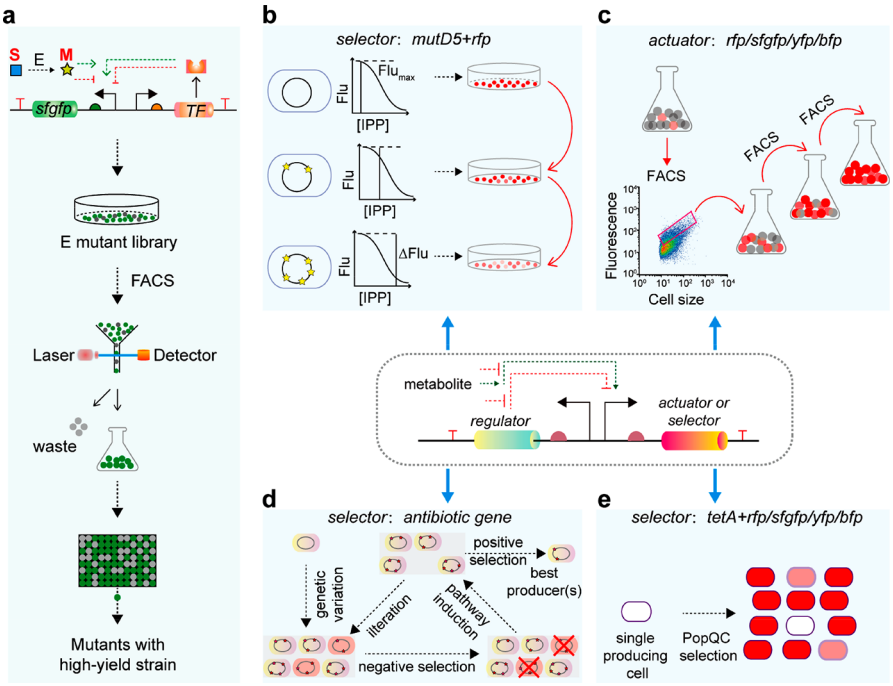

Figure 2. TFB-driven high-throughput screening and adaptive evolution systems. (a) High-throughput screening flow for high-yield strains. The constructed TFB was transformed into a mutant library to screen high-yield strains with FACS in multiwell plates. S, M, and E represent a substrate, target metabolite, and enzyme, respectively. Red blunt-ended dashed arrows denote repression, and green dashed arrows indicate activation. (b–e) TFB-based adaptive control systems. (b) Evolution of an isopentenyl pyrophosphate (IPP)-producing strain by using a feedback-regulated evolution of phenotype (FREP) strategy. In the absence of the ligand IPP, the biosensor activates the promoter, thus resulting in the expression of *mut*D5 and *rfp*. MutD5 increases the mutation rate, thereby resulting in the accumulation of mutations (yellow stars) on the chromosome (black circle) with each successive generation. Some mutations lead to increased IPP production and consequently decrease the ability of the biosensor to activate the expression of *mut*D5 and *rfp* in those cells. Flu represents fluorescence, and ΔFlu represents the change in fluorescence level. (c) Analysis of biosensor outputs for selecting evolutionary steps combined with FACS to construct artificial selection pressures to separate high-productivity variants. The biosensor cells were iteratively analyzed by FACS. 1 million cells were then isolated by gating on the top 10% fluorescence output, and sorted cells were iteratively recultivated and reisolated. (d) Switch selection scheme for biosynthetic pathway optimization through multiple rounds of evolution. "Cheaters" are eliminated to select optimal producers and improve target metabolite production. (e) Implementation of population quality control (PopQC) through continuously selecting high-performance and nongenetic variants and increasing their population representation. The high-performance biosensor activates the promoter controlling *tetA* and *rfp* expression, so that the cells can survive and dominate the population. White rounded rectangles represent low-performance cells, light-red rounded rectangles represent suboptimal performance cells. and red rounded rectangles represent high-performance cells.

promoters,[27] replication origins,[28] ribosome binding sites (RBSs),[29,30] transcription factor binding sites (TFBSs),[31,32] and TFs.[33−35] Traditional TFB engineering strategies mainly use trial-and-error approaches to optimize these regulatory elements.[33,36] However, through such approaches, predictable tuning of the TFB performance faces considerable challenges because of the unclear interaction mechanisms between TFB components.[37] Therefore, mathematical models, such as deep and machine learning, have been used to reprogram biological component databases, construct predictably tuned TFBs, and facilitate applications for metabolite monitoring and synthetically robust genetic circuits.[27]

Considering the critical roles of TFBs in metabolite engineering and synthetic biology, we first summarize the applications of TFBs. Then, on the basis of the limitations and problems that occur in these applications, we highlight the general requirements for efficient application: The TFB performance must be tuned according to individual demands. Beyond such tuning, the computer-assisted design of biological components and the automated design of genetic circuits can provide reasonable solutions to meet unresolved requirements. These approaches have changed considerably in recent years and have simultaneously improved the potential utility and impact of TFB engineering and accelerated the development of metabolic engineering and synthetic biology.

APPLICATIONS OF TFBS

In general, TFBs can be divided into two categories according to their TF type: (1) repressor-based and (2) activator-based biosensors (Figure 1a,b).[38] More specifically, the suppression function of the repressor can be activated or repressed when the inducer is present, thus resulting in the nonexpression or expression of target genes, respectively (Figure 1a).[39−41] In contrast, the activation function of the activator can be activated or repressed when the inducer is present, thus resulting in the expression or nonexpression of target genes, respectively (Figure 1b).[42−45] The expression of target genes is the output signal and is usually an externally detectable signal (such as fluorescence) or an undetectable signal (such as metabolic pathway regulation). The applications of TFBs can be categorized into four fields: metabolite measurement, high-throughput screening, adaptive evolution, and metabolic flux regulation. Herein we highlight some current applications of TFBs in metabolic engineering and synthetic biology.

Measurement of Target Metabolite Concentrations. In recent years, TFBs have been used to monitor real-time

https://doi.org/10.1021/acssynbio.0c00252
ACS Synth. Biol. XXXX, XXX, XXX−XXX

product formation, mainly unstable intracellular or trace target metabolite levels, such as CoA-thioesters and fatty acids (Table 1).[1] In this process, the input signal (concentration of the target metabolite) and the output signal (fluorescence) are used to establish dose−response curves, which can be used as standard curves to calculate target metabolite concentrations (Figure 1c). For example, Baumann *et al.* have developed a TFB for the rapid detection of short- and medium-chain fatty acids as a substitute for conventional gas chromatography.[47] Their TFB contains the P_{DR12} promoter, which responds to hexanoic acid, heptanoic acid, and caprylic acid in the linear ranges 0.01 to 2, 0.01 to 1.5, and 0.01 to 0.75 mM, respectively (Table 1).[47] The authors have also shown that the biosensor signal correlates strongly with the octanoic acid concentrations, as determined by gas chromatography, and have demonstrated the feasibility of TFB-based target metabolite measurement. Likewise, Chen *et al.* have developed and optimized a PuuR (native putrescine-responsive repressor protein)-based butadiamine biosensor, generating good response kinetics and detection ranges (Table 1).[48] They successfully used this biosensor to measure intracellular butadiamine concentrations in different engineered hosts and observed that secreted butadiamine levels strongly correlate with fluorescence intensity. Thus the sensor can detect butadiamine production during fermentation.[48] However, in establishing dose−response curves, researchers have often observed that TFBs no longer produce high fluorescence after the target metabolite concentrations exceed a particular threshold value called the detection range.[1,49] Thus designing TFBs with the desired performance is essential for detecting various metabolites.

High-Throughput Screening. TFBs have contributed to the establishment of high-throughput screening systems for biosensor-responsive metabolites. TFBs have been used with fluorescence-activated cell sorting (FACS) to rapidly screen high-yield strains from an extensive library (Figure 2a). For example, Li *et al.* developed a transcriptome-assisted metabolite-sensing (TAMES) strategy to identify sensor modules that respond to target metabolites.[58] The sensor modules were identified on the basis of selectivity between target metabolite-producing and nonproducing strains through comparative transcriptome analysis and RT-qPCR assessment. Finally, with this strategy, the 3-dehydroshikimate (DHS)-sensing module (CusR) was identified. The authors further constructed a CusR-based biosensor and established a high-throughput screening platform to screen high-yielding DHS strains, thus achieving a 90% enhancement in production.[58] This work provides a reference for the development of a novel TFB-based high-throughput screening platform. However, fluorescent protein expression usually generates an increasing burden on host cells, thus influencing the plasmid copy number and cell volume and further causing deviations in FACS screening.[9,12,59] Therefore, replacing reporters, such as antibiotic genes by automatically selecting superior producers from a library might alleviate this phenomenon.

TFB-Mediated Adaptive Evolution. TFB-mediated adaptive evolution is a powerful strategy for increasing metabolite production.[60,61] In this method, FACS or cell-dominant phenotype selection schemes repeatedly exert artificial selection pressure on TFB output, thus achieving the selection of specific high-yield strains. In the past decade, TFBs have attracted increasing attention owing to their applications in the adaptive evolution of production phenotypes. For example, Chou *et al.* have developed an adaptive control system for feedback-regulated evolution of phenotype (FREP). This approach couples the mutator (*mutD5*) and reporter to dynamically regulate the mutation rates in defective strains (Figure 2b).[45] Hence, the expression level of *mutD5* is positively associated with the mutation rate. The genomic mutation rate is inversely proportional to the concentration of intracellular isopentenyl pyrophosphate (IPP) on the basis of the FREP strategy. Thus the mutation rate decreases with increasing IPP, thereby stabilizing superior producers in populations.[45] The FREP strategy has been successfully applied to *E. coli*, and found to increase the biosynthesis of tyrosine and IPP by five and three times, respectively;[45] however, hundreds of single nucleotide polymorphisms were generated throughout the *E. coli* genome, thus increasing the complexity. To decrease the mutation rate, Mahr *et al.* established an adaptive laboratory evolution system by using artificial selection pressure in combination with an L-valine-responsive transcription factor (Lrp)-based biosensor and FACS[62] (Figure 2c). Through five iterative evolution steps, each transferring the 10% of cells with the highest fluorescence through FACS, the isolated *Corynebacterium glutamicum* variants showed a higher growth rate than that of the parental strain, with only seven mutations, and led to a 25% increase in L-valine production. Meanwhile, byproduct formation was reduced three- to four-fold.[62]

In general, high-throughput screening enriches for positive variants and eliminates negative variants. To eliminate "cheaters" in the evolutionary process, Raman *et al.* established a switching selection workflow[63] including iterative negative and positive selection steps to remove negative variants and enrich for positive variants (Figure 2d). The alternation between positive and negative selection pressures eliminates cheating in the population during each mutagenesis and screening round. When applied to the biosynthesis of naringenin and glucarate, this method has been found to increase production by 36- and 22-fold, respectively.[63] Beyond genetic performance, fermentation heterogeneity is another important phenomenon that significantly influences production.[12] This heterogeneity is caused by nongenetic cell-to-cell variations in gene expression and metabolite concentrations.[12,64] To limit the influence of fermentation heterogeneity, Xiao *et al.* developed a population quality-control system (PopQC) by using a free-fatty-acid-responsive TF (FadR)-based biosensor to continuously enrich for high producing cells and limit cells with inefficient production, thereby improving the population performance[64] (Figure 2e). PopQC effectively rewards high-performing cells with competitive cell growth advantages through the TFB output (*e.g.*, tetracycline resistance). The application of PopQC to tyrosine and fatty acid production has been found to increase yields by 2.6- and 3-fold, respectively.[64] Together, these examples demonstrate that TFB-driven adaptive evolution has played a crucial role in improving microbial metabolite production and accelerated adaptive evolution.

Dynamic Regulation of Metabolic Flux. Metabolic engineering consistently requires the redirection of metabolic flux into biosynthetic pathways without negatively influencing cell growth. However, growth conditions and individual intracellular states fluctuate during fermentation, thereby affecting the production of desired metabolites and impairing cell growth.[65] TFB-based dynamic regulation networks have been found to be beneficial in regulating metabolic flux in real time, according to changes in intracellular and extracellular

https://doi.org/10.1021/acssynbio.0c00252
ACS Synth. Biol. XXXX, XXX, XXX−XXX

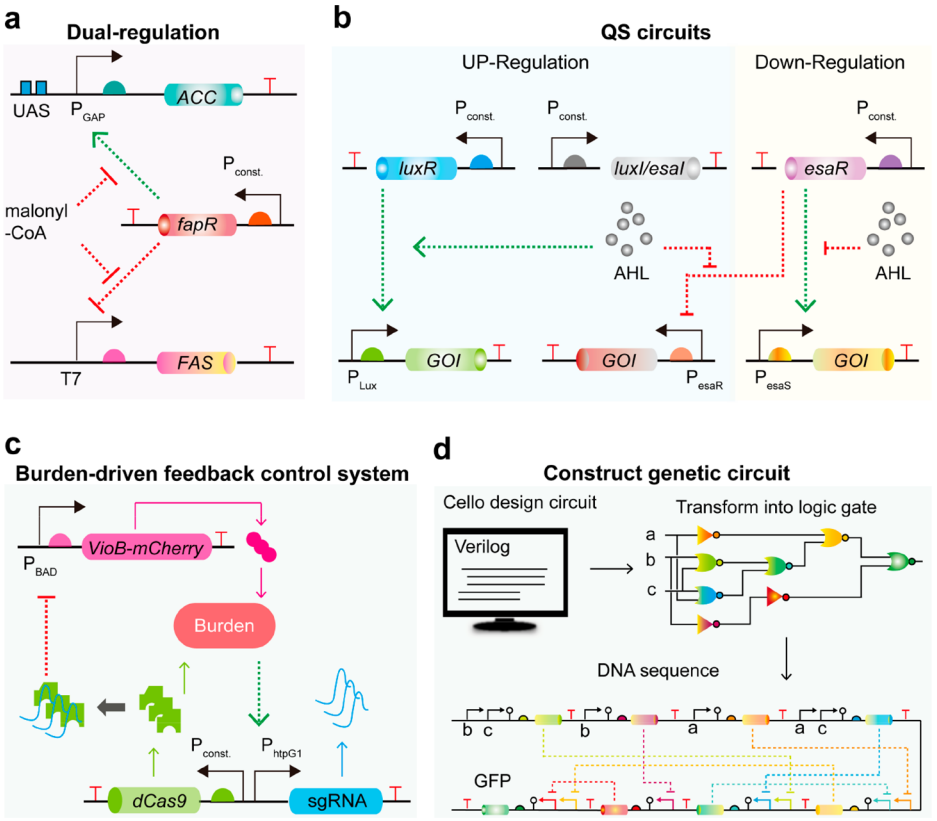

Figure 3. TFB-mediated dynamic regulation systems. (a) Dual-regulation system controlling the consumption and formation of malonyl-CoA. ACC, acetyl-CoA carboxylase; UAS, upstream activation sequence; P_{GAP}, *E. coli* P_{GAP} promoter; *fapR*, *B. subtilis* fatty acid pathway transcriptional regulator; P_{const}, constitutive promoter; T7, bacteriophage T7 promoter; FAS, fatty acid synthase. Red blunt-ended dashed arrows denote repression, and green dashed arrows indicate activation. (b) Regulation mechanism of the bifunctional QS system. As the cell density increases, AHL activates LuxR and alleviates the repression of EsaR, thus activating the expression of downstream genes controlled by the P_{Lux} and P_{easR} promoters. *GOI*, gene of interest; $P_{const.}$, constitutive promoter. Red blunt-ended dashed arrows denote repression, and green dashed arrows indicate activation. (c) Diagram of the burden-driven feedback control system. The *htpG1* promoter displays a strong on/off effect in burdened and unburdened cell states. This *htpG1* promoter has been used to control the expression of sgRNA, thus guiding dCas9 feedback-inhibition of target gene expression. P_{BAD}, *E. coli* arabinose-inducible promoter; $P_{const.}$, synthetic low-strength constitutive promoter; P_{htpG1}, *E. coli htpG* promoter. Red blunt-ended dashed arrows denote repression, and green dashed arrows indicate activation. (d) Construction of a genetic circuit with Cello. Design requirements for Cello are input with Verilog code, which is converted into a circuit diagram and subsequently into a DNA sequence representing the genetic circuit. $P_{const.}$ represents a constitutive promoter. The inputs a, b, and c correspond to sensor promoter activities. The genetic circuit consists of eight regulators (eight colors) and corresponding recognition promoters (eight corresponding colors). GFP, green fluorescent protein. Blunt-ended dashed arrows denote repression.

conditions. Malonyl-CoA is an essential precursor for cell growth and various value-added products, such as fatty acids and polyketides.[39,66,67] To balance biomass formation and compound production, Xu *et al.* and Liu *et al.* developed a malonyl-CoA dual-responsive TFB (Figure 3a) to dynamically regulate malonyl-CoA flux in cells and ultimately improve fatty acid biosynthesis.[39,68] Although these dynamic regulation modes effectively balance cell growth and product accumulation, production is still restricted by the limited metabolite-specific TFBs.[43] Hence, developing a universal TFB that could dynamically balance cell growth and the biosynthesis efficiency of discretionary metabolic pathways is critical for synthetic biology.

To establish a versatile dynamic control system, a process- and pathway-independent cell quorum-sensing (QS) control system has been used to control metabolic pathways, decouple cell growth, and target metabolite production processes[69] (Figure 3b). The *lux* system in *Vibrio fischeri* and the *esa* system in *Pantoea stewartia* are two well-studied QS systems. Gupta *et al.* established a pathway-independent dynamic control module (EsaI-EsaR) to regulate target gene expression at high cell densities.[70] In this module, the autoinducer 3-oxohexanoyl homoserine lactone (AHL) is produced by the synthase (EsaI), whose expression is controlled by the TF (EsaRI70 V), thus eliminating its activity. On the basis of the EsaI-EsaR module, a genetic circuit has been designed to tune EsaI expression levels and control phosphofructokinase-1 (*pfk-1*), and shikimate kinase (*aroK*) expression levels, thereby balancing the central metabolic pathway and the carbon flux of the target product synthesis.[70] This strategy has been found to significantly improve myo-inositol, glucarate, and shikimic acid production. Likewise, Dinh *et al.* constructed a bifunctional QS system containing two constitutively expressed regulatory proteins, EsaR and a 3-oxo-hexanoyl-homoserine lactone-responsive transcriptional activator (LuxR). LuxR and EsaR activate and repress the promoters P_{Lux} and P_{easR}, respectively.[71] When these proteins have been used to dynamically regulate naringenin and salicylic acid production pathways, the titer has been found to increase by 1.4- and 1.8-fold, respectively.[71]

https://doi.org/10.1021/acssynbio.0c00252
ACS Synth. Biol. XXXX, XXX, XXX−XXX

Table 2. Overview of TFB Performance

TFB	inducer	source	host	sensitivity	dynamic range	detection range
Repressor-based TFBs						
AcuR[54]	acrylate	*R. sphaeroides*	*E. coli*	3.2	90	0.016−10 mM
MphR[54]	erythromycin	*E. coli*	*E. coli*	1.6	108	0−1400 μM
TtgR[54]	naringenin	*P. putida*	*E. coli*	3.8	70	110−9000 μM
TetR[54]	anhydrotetracycline	*E. coli*	*E. coli*	4.2	63	0−430 nM
VanR[52]	vanillate	*C. crescentus*	*E. coli*	[a]	14.2	0.01−1 mM
BadR[85]	cyclohexanecarboxylate	*C. necator* H16	*C. necator* H16	1.11	11.4	0−1.25 mM
CsiR[22]	glutarate	*P. putida*	*E. coli*	1.61	1.5	0.005−0.0195 mM
BetI variant[41]	choline	*E. coli*	*E. coli*	1.3	49	0−100 mM
Activator-based TFBs						
CdaR[1,54]	glucarate	*E. coli*	*E. coli*	1	168	0−40 mM
AraC[54]	arabinose	*E. coli*	*E. coli*	1.3	210	0−40 mM
LuxR[86]	3OC6HSL	*V. fischeri*	*E. coli*	1.6	500	0.5−10 nM
OapR[85]	β-alanine	*C. necator* H16	*C. necator* H16	0.75	8.0	0−20 mM
FdsR[85]	formate	*C. necator* H16	*C. necator* H16	1.05	4.5	0−2.5 mM
XdhR[85]	xanthine	*C. necator* H16	*C. necator* H16	1.03	16.0	0−1 mM
PhgR[85]	phenylglyoxylate	*C. necator* H16	*C. necator* H16	0.96	144.8	0−5 mM
NahR[85]	salicylate	*C. necator* H16	*C. necator* H16	0.66	650.8	0−0.156 mM
BenM[85]	benzoate	*C. necator* H16	*C. necator* H16	1.64	74.1	0−1.25 mM
TtdR[85]	tartrate	*C. necator* H16	*C. necator* H16	0.80	370.6	0−150 mM
SauR[85]	sulfonatoacetate	*C. necator* H16	*C. necator* H16	0.57	395.4	0−10 mM
KynR[85]	L-kynurenine	*C. necator* H16	*C. necator* H16	0.98	26.9	0−0.625 mM
HpdR[85]	3-hydroxypropanoate	*C. necator* H16	*C. necator* H16	0.64	25.2	0−0.2 mM
PhhR[85]	L-phenylalanine	*C. necator* H16	*C. necator* H16	0.59	9.0	0−5 mM
HpdA[85]	L-tyrosine	*C. necator* H16	*C. necator* H16	0.72	38.3	0−0.156 mM
PcaQ[85]	3,4-dihydroxybenzoate	*C. necator* H16	*C. necator* H16	0.98	77.2	0−0.156 mM
AcoR[85]	acetoin	*C. necator* H16	*C. necator* H16	1.36	11.1	0−0.078 mM
GcdR[22]	glutarate	*P. putida*	*E. coli*	1.33	55.5	0.01−2.5 mM

[a]Not reported.

In general, synthetic biology approaches require the overexpression of exogenous genes to maximize metabolic flux, thereby consuming large amounts of building blocks and imposing a burden on cell growth. To solve this limitation, Ceroni *et al.* investigated the burden-responsive mechanism and constructed a burden-responsive TFB-based genetic circuit to regulate exogenous gene expression (Figure 3c).[49] The authors discovered a heat shock response protein-encoding gene, *htpG*, whose transcription levels are significantly elevated under a burden. The *htpG1* promoter senses the burden, and in response, an unknown effector represses the expression of "burdensome genes".[49] Hence, the *htpG1* promoter enables the construction of a feedback circuit balancing cell growth and exogenous gene expression. This approach has been found to alleviate metabolic burden, thus making engineered cells more competent for foreign gene expression at the population level.

Although many dynamic regulation networks have been established in the past decade, the complicated optimization process had hindered their application in metabolic engineering.[33,43] In this regard, strategies for rapid and precise dynamic regulation network construction and associated optimization could substantially promote biosynthesis. To this end, Cello was established for *in silico* genetic circuit design (Figure 3d).[72] With Cello, user-written source codes can be automatically converted into DNA sequences. Nielsen *et al.* used Cello to design 60 circuits for *E. coli*, 45 of which have been found to perform correctly in any output state (as many as 10 regulators and 55 parts).[72] The automated design has simplified the integration of genetic circuits in biotechnology projects requiring programmable control of biological functions or metabolite sensing[72] and has accelerated the application of dynamic control of metabolic flux.

TUNING TFB PERFORMANCE

Given the broad applications of TFBs, the design of robust and properly tuned TFBs is crucial to meet various application requirements. However, many wild-type and recombinant TFBs are hindered by low induction fold changes and high background noise.[21] These limitations may lead to undesired biosensor characteristics, such as low sensitivity, restricted dynamic range, poor specificity, limited detection ranges (Table 2),[5] and slow response times, thus requiring optimization.[38] Sensitivity distinguishes small differences in metabolite concentrations. The dynamic range evaluates the fold change in signal outputs. Specificity assesses the cross-talk between different metabolites. The detection range reveals the working concentration of TFBs. The response time reflects the signal-delaying levels of TFBs. With a focus on this performance, we highlight several TFB engineering strategies to provide a guide for generating optimal biosensors. The TFB performance is summarized in Table 2.

Promoter, Replication Origin, and RBS Engineering to Tune the Dose−Response Properties of TFBs. In general, the dynamic range, sensitivity, and detection range are considered dose−response properties because they are associated with inducer concentrations and output signals. In practice, most TFBs with optimal response performance have been generated *via* traditional trial-and-error experiments.[25] One of the most commonly used strategies is promoter optimization or engineering, which regulates the transcription

https://doi.org/10.1021/acssynbio.0c00252
ACS Synth. Biol. XXXX, XXX, XXX−XXX

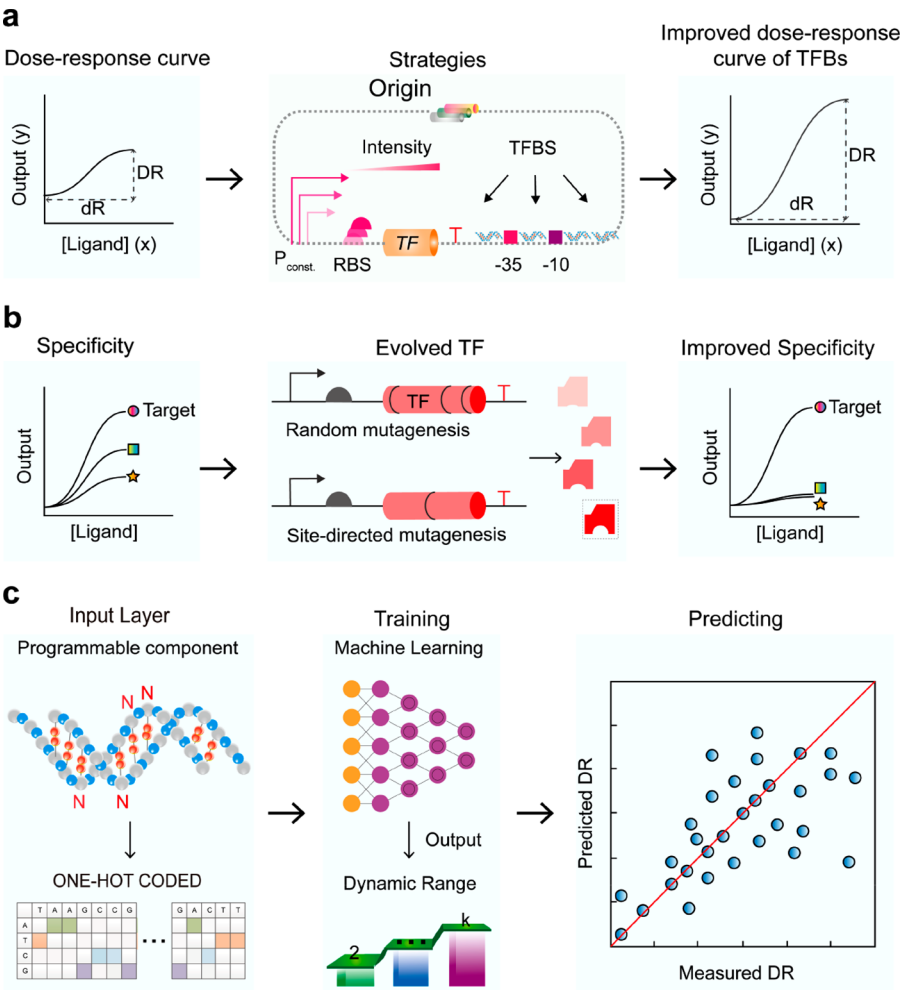

Figure 4. Strategies for tuning the TFB performance. (a) Dose−response curves of the TFB have been tuned through various strategies, such as promoter, RBS, and TFBS engineering, to obtain the desired sensitivity (Hill coefficient of fitted x and y data), detection range (dR, horizontal double gray dashed arrow), and dynamic range (DR, vertical double gray dashed arrow). $P_{const.}$ represents the constitutive promoter. (b) Protein engineering strategy to modify the specificity of TFBs. A transcription factor variant responding to only the target metabolite was obtained through random or site-directed mutation (red TF in dashed box). Red circle, target ligand; green square and orange stars, other ligands; black curve on the cylinder, mutation sites. (c) Computer-assisted TFB rational design strategies. A programmable component that tunes the dynamic range of the TFB was designed and used to generate a predictable TFB according to a machine-learning model. N represents arbitrary bases. These components were converted into pictures through one-hot encoding and used as the input layer in machine learning, and the dynamic ranges were used as the output. Through continuous training of the model, a predictive model with good performance was developed and found to achieve fast and accurate prediction of the dynamic range.

levels of TFs or reporters (Figure 4a). This regulation not only influences the inducer binding ability but also affects TFBS binding, thus achieving an optimized and regulated dynamic range, sensitivity, and detection range. For example, Thompson *et al.* screened a high-sensitivity valerolactam and caprolactam biosensor based on the oxoprolinase regulator (OplR) from *Pseudomonas putida* KT2440 through optimizing the promoter of OplR.[73] The authors combined a reporter gene and a regulatory gene and constructed the pLACSENS plasmid family by using promoters with different strengths. The valerolactam data revealed that the moderate-intensity promoter-controlled sensor pLACSENS3 yielded the highest sensitivity and low detection limits (<12 nM); however, the high-intensity promoter-controlled sensor pLACSENS5 generated the lowest sensitivity and high detection limits (1.5 μM).[73] The high sensitivity and detection range of the OplR-based biosensor were influential in developing novel caprolactam biosynthetic routes. Furthermore, engineering of the promoters driving the reporter enabled the biosensor's dynamic range to be adjusted to achieve the desired "on" and "off" characteristics. To obtain TFBs with the desired induction and leakage expression levels, Chen *et al.* constructed a set of synthetic promoters to control reporter expression by combining different −10 and −35 boxes with different equilibrium constants (K_{eq}) of σ^{70} binding to DNA.[74] A dynamic range of ∼10^4-fold was achieved by using synthetic promoters to optimize the AraC- or LasR-regulated biosensors.

According to TFB mechanisms (Figure 1a,b), TF binding to ligands and TFBSs plays a critical role in biosensor performance. Therefore, Chen *et al.* assembled a hybrid promoter to strictly control gene expression through multi-ligand input.[74] The hybrid promoters contain two operating sequences upstream of the −35 sites (TFBSs of AraC or XylR) and between the −10 and −35 sites (TFBSs of LacI or TetR). All combinations of hybrid promoters have been found to exhibit high-efficiency induction only in the presence of two

https://doi.org/10.1021/acssynbio.0c00252
ACS Synth. Biol. XXXX, XXX, XXX−XXX

inducers.[74] Ultimately, this design ensures strict regulation of the dynamic range of hybrid promoters. In addition, adjusting the numbers and positions of TFBSs to establish optimized promoters significantly affects the TFB dose response (Figure 4a). For example, 14 inducible promoters have been constructed by inserting the TFBS (gamO2) of GamR, a TF that responds to glucosamine-6-phosphate (GlcN6P), at the two sides or spacer positions of the −35 and −10 regions of the constitutive promoter P_{veg}.[75] Finally, the use of these promoters to optimize the GlcN6P-responsive biosensor resulted in significantly decreased basal expression, and the dynamic range improved to 13.4-fold.[75] Alternatively, TF and reporter gene expression can be regulated by plasmid copy number engineering. For example, Thompson *et al.* obtained multiple mutations from the DNA helicase RepA that increased the copy number of the pSC101 origin of replication containing plasmids, thereby increasing the sensitivity of ChnR (lactam-responsive AraC-family protein)-based biosensors.[76]

Promoter and plasmid copy number engineering have mainly focused on regulating the transcriptional level of the TF and reporter to fine-tune the performance of the TFB.[74] At the translation level, a key element regulating the TFB performance is the RBS, which tunes TFB dose−response properties by adjusting the translation levels of the TF and reporter (Figure 4a). For example, Siedler *et al.* identified PadR, a transcription repressor that naturally responds to *p*-coumaric acid.[77] However, the low expression concentration of PadR in cells is insufficient to suppress the expression inducible promoter.[77] Therefore, to construct a robust biosensor, an optimal PadR expression level was obtained by randomly mutating the RBS of PadR, and the dynamic range improved to 130-fold in the presence of *p*-coumaric acid after high-throughput screening.[77] However, random mutation and screening of the optimal RBS is a time-consuming and laborious process. Standard RBS components with specific characteristics have been developed, which can be optimized and tested quickly and can easily be replaced, thereby improving the speed of optimization.[78] Furthermore, deep-learning models can now be used to rapidly predict a biosensor's dynamic range corresponding to a specific RBS sequence.[37]

TF Engineering to Tune the Specificity of a TFB. Another critical property of TFBs is specificity, which is generally determined by the TF structure. Thus most studies have focused on protein engineering to rationally or randomly adjust protein structure (Figure 4b). For example, Li *et al.* successfully shifted the specificity of the uric-acid-responsive TF HucR to shikimic acid by introducing saturation mutations affecting ligand binding pocket residues.[79] To further extend the specificity of HucR, Liang *et al.* performed site-directed saturation mutagenesis to significantly decrease and enhance the response to ferulic acid and vanillin, respectively.[80] However, screening positive mutants from a large library is often time-consuming and laborious, thus hindering the application of such mutation strategies. To overcome this challenge, Collins *et al.* used a dual-selection system to select for LuxR variants that either activate or repress gene expression under the desired conditions.[81] The identified variant, LuxR-G2E, retained its response to straight-chain acyl-homoserine lactones but no longer responded to 3-oxo-hexanoyl-homoserine lactone, thereby improving the specificity. More information on dose−responses and specificity enhancements can be found in a review by Koch *et al.* describing other strategies (*e.g.*, the construction of chimeric TFs) for modifying the TFB performance in response to a given ligand.[33]

Computer-Assisted Tuning Approaches. Although traditional trial-and-error engineering strategies have made substantial advances, they are both time- and labor-consuming. To overcome these limitations, the rational design of TFBs with the desired performance is a promising novel approach that is expected to gain popularity. The necessary exploration of the quantitative relationships among the inducer concentration, TF, reporter expression levels, and TFBS positions as well as the analysis of the underlying mechanisms is highly challenging with current technology.[82] To bypass these challenges, mathematical models, such as deep and machine learning,[83] which do not require in-depth knowledge of internal TFB mechanisms, have been combined with large databases to predict the TFB performance (Figure 4c). Deep learning is an algorithm that uses artificial neural networks (*e.g.*, convolutional neural networks and recurrent neural networks) as a framework to characterize and learn data. Machine learning uses algorithms (*e.g.*, Naive Bayes, Support Vector Machines, or Logistic Regression) to mine the hidden rules and essence of things to obtain a model through data training.[27,84] Therefore, to reprogram TFBs to generate predictable performance, Liu *et al.* designed an inducible promoter *de novo* by embedding TFBSs of varying affinities within a minimal constitutive *E. coli* promoter. A cell-free system was used to iteratively screen and enrich inducible TF-bound promoters *via* high-throughput *in vivo* sorting.[27] The sorted promoters were analyzed and formed a data set that was used to train a machine-learning model that predicted dynamic ranges with a given promoter sequence. The data revealed that although TFBSs are necessary for TF binding, the relative position and base sequences on both sides of the TFBS play essential roles in regulating the TFB performance.[27]

Furthermore, the RBS influences the dynamic range of the TFB by controlling the translation level of the TF and the reporter. The translation rate further affects the protein activity and folding states.[37] Hence the complicated interactions between the translation level and folding states of the TF and reporter pose challenges in tuning the dynamic range through RBS engineering. In this context, we developed a classification model (CLM-RDR) involving the RBS and the dynamic range of the TFB.[37] Using this model, we successfully predicted the dynamic range of a glucarate-responsive biosensor with an accuracy of 72.2%.[37]

Tuning the Response Time of a TFB. Owing to the chemical transportation, gene transcription, and protein translation, TFBs have inherent limitations due to slow response times,[5,20] thus leading to signal distortions and delays during metabolic flux regulation.[87] The fast response time of a TFB allows for real-time monitoring of environmental changes and accurate regulation of the cellular metabolic flux.[5] Hence a shortened response time is critical for synchronizing environmental changes and phenotype formation.[11] Given that whole-cell biosensor uptake of extracellular target chemicals is the first step in triggering output, response times can be adjusted by changing the culture medium.[48] Furthermore, several natural TFs, such as AraC, have a negative autoregulation (NAR) function that shortens response times, thus enabling a response steady state, decreasing noise and tuning the input−output response curve by balancing TF levels.[26] For example, Madar *et al.* have shown that the response time is shorter when the TF is

https://doi.org/10.1021/acssynbio.0c00252
ACS Synth. Biol. XXXX, XXX, XXX−XXX

negatively autoregulated. This phenomenon has been observed in a synthetic NAR circuit in *E. coli*. The function of shortening response time provided by NAR might be advantageous in producing a fast response in a dynamic environment, wherein the rapid response improves the fitness.[26]

However, the expressed reporters or TFs are likely to exist for several hours in cells,[7] thereby influencing the real-time signal transition and failing to eliminate the metabolic burden caused by the numerous expressed proteins. Hence degradation of the expressed TFs and reporters in a timely manner is crucial to avoid signal delay. The protein degradation tag SsrA is often added to the C-terminus of the TFB reporter or the TF to ensure that the translated proteins have short half lives,[70] and dynamic changes in the metabolites can be detected across different time points. Degradation tags provide additional control mechanisms for regulating protein pools and pathway flux in cells. Phenotypic changes such as adjustments to response properties can be accurately observed by eliminating the protein pool of reporters in the cells.[70]

Overall, high-performance tunable TFBs can be generated *via* a series of strategies, such as promoter and RBS optimization or engineering, plasmid copy number optimization, TF engineering, and computer-assisted engineering. These methods allow TFBs to respond to target metabolites with optimal dose−response properties and high specificity. In addition, tunable TFBs contribute to the accurate measurement of metabolite concentrations and have provided a robust knowledge base for the design of complex gene circuit networks. In the future, the design of superior TFBs is expected to expand the knowledge base for research groups, thus increasing the tunable application of biosensors in metabolic engineering and synthetic biology.

CONCLUSIONS AND PROSPECTS

TFBs have been successfully used for high-throughput screening of high-yield strains and to control pathway dynamics.[39,68,88,89] Tunable TFBs have been used to construct synthetic biology devices with superior performance while circumventing tedious and time-consuming metabolite production detection.[50] Furthermore, they have also enabled the accurate design of robust genetic circuits such as logic gates[72] and ring oscillators.[90] Despite major success in tuning the TFB performance through various strategies,[26,91] predicting the performance and developing metabolic engineering applications remain challenging. To overcome these limitations, large data mining of biological components, combined with powerful mathematical models such as deep learning and machine learning, will be helpful in the rational design of genetic circuits and TFBs. In this scenario, thousands of TFBs with different phenotypes and biological components must be constructed and characterized to collect data for training mathematical models—a process that can be challenging. The analysis and verification of the physical phenotypic changes produced by each mathematical model require extensive data support and the services of professional mathematicians. Understanding and demonstrating the complicated interactions and regulatory mechanisms among promoters, RBSs, regulators, and reporters on the TFB performance, such as how biological regulatory elements affect downstream protein folding,[37] will lay a solid foundation for the rational design of tunable TFBs.[82] Overall, we believe that interdisciplinary work will help overcome these issues.[92]

AUTHOR INFORMATION

Corresponding Authors

Yu Deng − *National Engineering Laboratory for Cereal Fermentation Technology (NELCF) and Jiangsu Provincial Research Center for Bioactive Product Processing Technology, Jiangnan University, Wuxi, Jiangsu 214122, China*; orcid.org/0000-0002-1909-7223; Email: dengyu@jiangnan.edu.cn

Shenghu Zhou − *National Engineering Laboratory for Cereal Fermentation Technology (NELCF) and Jiangsu Provincial Research Center for Bioactive Product Processing Technology, Jiangnan University, Wuxi, Jiangsu 214122, China*; Email: zhoush@jiangnan.edu.cn

Author

Nana Ding − *National Engineering Laboratory for Cereal Fermentation Technology (NELCF) and Jiangsu Provincial Research Center for Bioactive Product Processing Technology, Jiangnan University, Wuxi, Jiangsu 214122, China*

Complete contact information is available at: https://pubs.acs.org/10.1021/acssynbio.0c00252

Author Contributions

Y.D. and S.Z. designed the manuscript. N.D. wrote the manuscript. Y.D. and S.Z. critically revised the manuscript. All authors reviewed, approved, and contributed to the final version of the manuscript.

Notes

The authors declare no competing financial interest.

ACKNOWLEDGMENTS

This work was supported by the National Key R&D Program of China (2019YFA0905500), the National Natural Science Foundation of China (21877053, 31900066), the Fundamental Research Funds for the Central Universities (JUSRP51705A, JUSRP11964), and the National First-class Discipline Program of Light Industry Technology and Engineering (LITE2018-24).

KEY CONCEPTS

Sensitivity, Hill coefficient of the fitted dose curve, describing the changes in speed of the output signal when the ligand concentration transitions from low to high; Specificity, the relative difference between the increased output signal after target ligand binding and the output signal for the binding of other potential ligands of interest; Dynamic range, fold change in gene expression between the presence and absence of an inducer; Detection range, the range between the lower and upper limits of measured inducer values; Response time, the time when the signal reaches half the highest output signal after induction

REFERENCES

(1) Rogers, J. K., and Church, G. M. (2016) Genetically encoded sensors enable real-time observation of metabolite production. *Proc. Natl. Acad. Sci. U. S. A. 113* (9), 2388−2393.

(2) Peters, G., De Paepe, B., De Wannemaeker, L., Duchi, D., Maertens, J., Lammertyn, J., and De Mey, M. (2018) Development of N-acetylneuraminic acid responsive biosensors based on the transcriptional regulator NanR. *Biotechnol. Bioeng. 115* (7), 1855−1865.

(3) Rebets, Y., Schmelz, S., Gromyko, O., Tistechok, S., Petzke, L., Scrima, A., and Luzhetskyy, A. (2018) Design, development and

application of whole-cell based antibiotic-specific biosensor. *Metab. Eng. 47*, 263−270.
(4) Wang, Q. Z., Tang, S. Y., and Yang, S. (2017) Genetic biosensors for small-molecule products: Design and applications in high-throughput screening. *Front. Chem. Sci. Eng. 11* (1), 15−26.
(5) Carpenter, A. C., Paulsen, I. T., and Williams, T. C. (2018) Blueprints for biosensors: design, limitations, and applications. *Genes 9* (8), 375.
(6) van der Helm, E., Genee, H. J., and Sommer, M. O. A. (2018) The evolving interface between synthetic biology and functional metagenomics. *Nat. Chem. Biol. 14* (8), 752−759.
(7) Zhang, L. Y., Guo, W., and Lu, Y. (2020) Advances in cell-free biosensors: Principle, mechanism, and applications. *Biotechnol. J. 15* (9), 2000187.
(8) Wan, X. Y., Volpetti, F., Petrova, E., French, C., Maerkl, S. J., and Wang, B. J. (2019) Cascaded amplifying circuits enable ultrasensitive cellular sensors for toxic metals. *Nat. Chem. Biol. 15* (5), 540−548.
(9) Yang, D., Park, S. Y., Park, Y. S., Eun, H., and Lee, S. Y. (2020) Metabolic engineering of *Escherichia coli* for natural product biosynthesis. *Trends Biotechnol. 38* (7), 745−765.
(10) Zeng, W. Z., Guo, L. K., Xu, S., Chen, J., and Zhou, J. W. (2020) High-throughput screening technology in industrial biotechnology. *Trends Biotechnol. 38* (8), 888−906.
(11) Shen, X. L., Wang, J., Li, C. Y., Yuan, Q. P., and Yan, Y. J. (2019) Dynamic gene expression engineering as a tool in pathway engineering. *Curr. Opin. Biotechnol. 59*, 122−129.
(12) Rugbjerg, P., and Sommer, M. O. A. (2019) Overcoming genetic heterogeneity in industrial fermentations. *Nat. Biotechnol. 37* (8), 869−876.
(13) Lv, Y. K., Qian, S., Du, G. C., Chen, J., Zhou, J. W., and Xu, P. (2019) Coupling feedback genetic circuits with growth phenotype for dynamic population control and intelligent bioproduction. *Metab. Eng. 54*, 109−116.
(14) Bowman, E. K., and Alper, H. S. (2020) Microdroplet-assisted screening of biomolecule production for metabolic engineering applications. *Trends Biotechnol. 38* (7), 701−714.
(15) Sandberg, T. E., Salazar, M. J., Weng, L. L., Palsson, B. O., and Feist, A. M. (2019) The emergence of adaptive laboratory evolution as an efficient tool for biological discovery and industrial biotechnology. *Metab. Eng. 56*, 1−16.
(16) Xu, X. H., Li, X. L., Liu, Y. F., Zhu, Y. L., Li, J. H., Du, G. C., Chen, J., Ledesma-Amaro, R., and Liu, L. (2020) Pyruvate-responsive genetic circuits for dynamic control of central metabolism. *Nat. Chem. Biol. 16* (11), 1261−1268.
(17) Stephens, K., Pozo, M., Tsao, C. Y., Hauk, P., and Bentley, W. E. (2019) Bacterial co-culture with cell signaling translator and growth controller modules for autonomously regulated culture composition. *Nat. Commun. 10* (1), 4129.
(18) Chen, S. Y., Wei, W. P., Yin, B. C., Tong, Y. B., Lu, J. J., and Ye, B. C. (2019) Development of a highly sensitive whole-cell biosensor for arsenite detection through engineered promoter modifications. *ACS Synth. Biol. 8* (10), 2295−2302.
(19) Wan, X., Marsafari, M., and Xu, P. (2019) Engineering metabolite-responsive transcriptional factors to sense small molecules in eukaryotes: current state and perspectives. *Microb. Cell Fact. 18* (1), 61.
(20) Grazon, C., Baer, R. C., Kuzmanović, U., Nguyen, T., Chen, M., Zamani, M., Chern, M., Aquino, P., Zhang, X. M., Lecommandoux, S., Fan, A., Cabodi, M., Klapperich, C., Grinstaff, M. W., Dennis, A. M., and Galagan, J. E. (2020) A progesterone biosensor derived from microbial screening. *Nat. Commun. 11* (1), 1276.
(21) De Paepe, B., Peters, G., Coussement, P., Maertens, J., and De Mey, M. (2017) Tailor-made transcriptional biosensors for optimizing microbial cell factories. *J. Ind. Microbiol. Biotechnol. 44*, 623−645.
(22) Thompson, M. G., Costello, Z., Hummel, N. F. C., Cruz-Morales, P., Blake-Hedges, J. M., Krishna, R. N., Skyrud, W., Pearson, A. N., Incha, M. R., Shih, P. M., Garcia-Martin, H., and Keasling, J. D. (2019) Robust characterization of two distinct glutarate sensing transcription factors of *Pseudomonas putida* l-lysine metabolism. *ACS Synth. Biol. 8* (10), 2385−2396.
(23) Dietrich, J. A., Shis, D. L., Alikhani, A., and Keasling, J. D. (2013) Transcription factor-based screens and synthetic selections for microbial small-molecule biosynthesis. *ACS Synth. Biol. 2* (1), 47−58.
(24) Cheng, F., Tang, X. L., and Kardashliev, T. (2018) Transcription factor-based biosensors in high-throughput screening: advances and applications. *Biotechnol. J. 13* (7), 1700648.
(25) Johnson, A. O., Gonzalez-Villanueva, M., Wong, L., Steinbüchel, A., Tee, K. L., Xu, P., and Wong, T. S. (2017) Design and application of genetically-encoded malonyl-CoA biosensors for metabolic engineering of microbial cell factories. *Metab. Eng. 44*, 253−264.
(26) Madar, D., Dekel, E., Bren, A., and Alon, U. (2011) Negative auto-regulation increases the input dynamic-range of the arabinose system of *Escherichia coli*. *BMC Syst. Biol. 5*, 111.
(27) Liu, X. Y., Gupta, S. T. P., Bhimsaria, D., Reed, J. L., Rodríguez-Martínez, J. A., Ansari, A. Z., and Raman, S. (2019) De novo design of programmable inducible promoters. *Nucleic Acids Res. 47* (19), 10452−10463.
(28) Lim, H. G., Jang, S., Jang, S., Seo, S. W., and Jung, G. Y. (2018) Design and optimization of genetically encoded biosensors for high-throughput screening of chemicals. *Curr. Opin. Biotechnol. 54*, 18−25.
(29) Yeom, S. J., Kim, M., Kwon, K. K., Fu, Y. Y., Rha, E., Park, S. H., Lee, H., Kim, H., Lee, D. H., Kim, D. M., and Lee, S. G. (2018) A synthetic microbial biosensor for high-throughput screening of lactam biocatalysts. *Nat. Commun. 9* (1), 5053.
(30) Kalkreuter, E., Keeler, A. M., Malico, A. A., Bingham, K. S., Gayen, A. K., and Williams, G. J. (2019) Development of a genetically encoded biosensor for detection of polyketide synthase extender units in *Escherichia coli*. *ACS Synth. Biol. 8* (6), 1391−1400.
(31) Snoek, T., Chaberski, E. K., Ambri, F., Kol, S., Bjørn, S. P., Pang, B., Barajas, J. F., Welner, D. H., Jensen, M. K., and Keasling, J. D. (2020) Evolution-guided engineering of small-molecule biosensors. *Nucleic Acids Res. 48* (1), e3.
(32) Juárez, J. F., Lecube-Azpeitia, B., Brown, S. L., Johnston, C. D., and Church, G. M. (2018) Biosensor libraries harness large classes of binding domains for construction of allosteric transcriptional regulators. *Nat. Commun. 9* (1), 3101.
(33) Koch, M., Pandi, A., Borkowski, O., Batista, A. C., and Faulon, J. L. (2019) Custom-made transcriptional biosensors for metabolic engineering. *Curr. Opin. Biotechnol. 59*, 78−84.
(34) Szenk, M., Yim, T., and Balázsi, G. (2020) Multiplexed gene expression tuning with orthogonal synthetic gene circuits. *ACS Synth. Biol. 9* (4), 930−939.
(35) Rondon, R. E., Groseclose, T. M., Short, A. E., and Wilson, C. J. (2019) Transcriptional programming using engineered systems of transcription factors and genetic architectures. *Nat. Commun. 10* (1), 4784.
(36) Hossain, G. S., Saini, M., Miyake, R., Ling, H., and Chang, M. W. (2020) Genetic biosensor design for natural product biosynthesis in microorganisms. *Trends Biotechnol. 38* (7), 797−810.
(37) Ding, N. N., Yuan, Z. Q., Zhang, X. J., Chen, J., Zhou, S. H., and Deng, Y. (2020) Programmable cross-ribosome-binding sites to fine-tune the dynamic range of transcription factor-based biosensor. *Nucleic Acids Res. 48* (18), 10602−10613.
(38) Mannan, A. A., Liu, D., Zhang, F. Z., and Oyarzún, D. A. (2017) Fundamental design principles for transcription-factor-based metabolite biosensors. *ACS Synth. Biol. 6* (10), 1851−1859.
(39) Xu, P., Li, L. Y., Zhang, F. M., Stephanopoulos, G., and Koffas, M. (2014) Improving fatty acids production by engineering dynamic pathway regulation and metabolic control. *Proc. Natl. Acad. Sci. U. S. A. 111* (31), 11299−11304.
(40) Xu, P. (2018) Production of chemicals using dynamic control of metabolic fluxes. *Curr. Opin. Biotechnol. 53*, 12−19.
(41) Saeki, K., Tominaga, M., Kawai-Noma, S., Saito, K., and Umeno, D. (2016) Rapid diversification of BetI-based transcriptional switches for the control of biosynthetic pathways and genetic circuits. *ACS Synth. Biol. 5* (11), 1201−1210.

https://doi.org/10.1021/acssynbio.0c00252
ACS Synth. Biol. XXXX, XXX, XXX−XXX

(42) Wang, B. J., Barahona, M., and Buck, M. (2015) Amplification of small molecule-inducible gene expression via tuning of intracellular receptor densities. *Nucleic Acids Res. 43* (3), 1955−1964.
(43) Mahr, R., and Frunzke, J. (2016) Transcription factor-based biosensors in biotechnology: current state and future prospects. *Appl. Microbiol. Biotechnol. 100* (1), 79−90.
(44) Hanko, E. K. R., Minton, N. P., and Malys, N. (2018) A transcription factor-based biosensor for detection of itaconic acid. *ACS Synth. Biol. 7* (5), 1436−1446.
(45) Chou, H. H., and Keasling, J. D. (2013) Programming adaptive control to evolve increased metabolite production. *Nat. Commun. 4*, 2595.
(46) Pédelacq, J. D., Cabantous, S., Tran, T., Terwilliger, T. C., and Waldo, G. S. (2006) Engineering and characterization of a superfolder green fluorescent protein. *Nat. Biotechnol. 24* (1), 79−88.
(47) Baumann, L., Rajkumar, A. S., Morrissey, J. P., Boles, E., and Oreb, M. (2018) A yeast-based biosensor for screening of short-and medium-chain fatty acid production. *ACS Synth. Biol. 7* (11), 2640−2646.
(48) Chen, X. F., Xia, X. X., Lee, S. Y., and Qian, Z. G. (2018) Engineering tunable biosensors for monitoring putrescine in *Escherichia coli*. *Biotechnol. Bioeng. 115* (4), 1014−1027.
(49) Ceroni, F., Boo, A., Furini, S., Gorochowski, T. E., Borkowski, O., Ladak, Y. N., Awan, A. R., Gilbert, C., Stan, G. B., and Ellis, T. (2018) Burden-driven feedback control of gene expression. *Nat. Methods 15* (5), 387−393.
(50) Skjoedt, M. L., Snoek, T., Kildegaard, K. R., Arsovska, D., Eichenberger, M., Goedecke, T. J., Rajkumar, A. S., Zhang, J., Kristensen, M., Lehka, B. J., Siedler, S., Borodina, I., Jensen, M. K., and Keasling, J. D. (2016) Engineering prokaryotic transcriptional activators as metabolite biosensors in yeast. *Nat. Chem. Biol. 12* (11), 951−958.
(51) Kim, S. K., Kim, S. H., Subhadra, B., Woo, S. G., Rha, E., Kim, S. W., Kim, H., Lee, D. H., and Lee, S. G. (2018) A genetically encoded biosensor for monitoring isoprene production in engineered *Escherichia coli*. *ACS Synth. Biol. 7* (10), 2379−2390.
(52) Kunjapur, A. M., and Prather, K. L. J. (2019) Development of a vanillate biosensor for the vanillin biosynthesis pathway in *E. coli*. *ACS Synth. Biol. 8* (9), 1958−1967.
(53) Zhang, F. Z., Carothers, J. M., and Keasling, J. D. (2012) Design of a dynamic sensor-regulator system for production of chemicals and fuels derived from fatty acids. *Nat. Biotechnol. 30* (4), 354−359.
(54) Rogers, J. K., Guzman, C. D., Taylor, N. D., Raman, S., Anderson, K., and Church, G. M. (2015) Synthetic biosensors for precise gene control and real-time monitoring of metabolites. *Nucleic Acids Res. 43* (15), 7648−7660.
(55) Zhang, J. W., Barajas, J. F., Burdu, M., Ruegg, T. L., Dias, B., and Keasling, J. D. (2017) Development of a transcription factor based lactam biosensor. *ACS Synth. Biol. 6* (3), 439−445.
(56) Kasey, C. M., Zerrad, M., Li, Y. W., Cropp, T. A., and Williams, G. J. (2018) Development of transcription factor-based designer macrolide biosensors for metabolic engineering and synthetic biology. *ACS Synth. Biol. 7* (1), 227−239.
(57) Lin, C., Jair, Y. C., Chou, Y. C., Chen, P. S., and Yeh, Y. C. (2018) Transcription factor-based biosensor for detection of phenylalanine and tyrosine in urine for diagnosis of phenylketonuria. *Anal. Chim. Acta 1041*, 108−113.
(58) Li, L. P., Tu, R., Song, G. T., Cheng, J., Chen, W. J., Li, L., Wang, L. X., and Wang, Q. H. (2019) Development of a synthetic 3-dehydroshikimate biosensor in *Escherichia coli* for metabolite monitoring and genetic screening. *ACS Synth. Biol. 8* (2), 297−306.
(59) Zhou, S. H., Ding, R. P., Chen, J., Du, G. C., Li, H. Z., and Zhou, J. W. (2017) Obtaining a panel of cascade promoter-5 ′-UTR complexes in *Escherichia coli*. *ACS Synth. Biol. 6* (6), 1065−1075.
(60) Stella, R. G., Wiechert, J., Noack, S., and Frunzke, J. (2019) Evolutionary engineering of *Corynebacterium glutamicum*. *Biotechnol. J. 14* (9), 1800444.
(61) Liu, S. D., Wu, Y. N., Wang, T. M., Zhang, C., and Xing, X. H. (2017) Maltose utilization as a novel selection strategy for continuous evolution of microbes with enhanced metabolite production. *ACS Synth. Biol. 6* (12), 2326−2338.
(62) Mahr, R., Gätgens, C., Gätgens, J., Polen, T., Kalinowski, J., and Frunzke, J. (2015) Biosensor-driven adaptive laboratory evolution of l-valine production in *Corynebacterium glutamicum*. *Metab. Eng. 32*, 184−194.
(63) Raman, S., Rogers, J. K., Taylor, N. D., and Church, G. M. (2014) Evolution-guided optimization of biosynthetic pathways. *Proc. Natl. Acad. Sci. U. S. A. 111* (50), 17803−17808.
(64) Xiao, Y., Bowen, C. H., Liu, D., and Zhang, F. Z. (2016) Exploiting nongenetic cell-to-cell variation for enhanced biosynthesis. *Nat. Chem. Biol. 12* (5), 339−344.
(65) Choe, D., Lee, J. H., Yoo, M., Hwang, S., Sung, B. H., Cho, S., Palsson, B., Kim, S. C., and Cho, B. K. (2019) Adaptive laboratory evolution of a genome-reduced *Escherichia coli*. *Nat. Commun. 10* (1), 935.
(66) Zhou, S. H., Hao, T. T., Xu, S. M., and Deng, Y. (2020) Coenzyme A thioester-mediated carbon chain elongation as a paintbrush to draw colorful chemical compounds. *Biotechnol. Adv. 43*, 107575.
(67) Liu, L. X., Zhou, S. H., and Deng, Y. (2020) The 3-ketoacyl-CoA thiolase: an engineered enzyme for carbon chain elongation of chemical compounds. *Appl. Microbiol. Biotechnol. 104* (19), 8117−8129.
(68) Liu, D., Xiao, Y., Evans, B. S., and Zhang, F. Z. (2015) Negative feedback regulation of fatty acid production based on a malonyl-CoA sensor-actuator. *ACS Synth. Biol. 4* (2), 132−140.
(69) Doong, S. J., Gupta, A., and Prather, K. L. J. (2018) Layered dynamic regulation for improving metabolic pathway productivity in *Escherichia coli*. *Proc. Natl. Acad. Sci. U. S. A. 115* (12), 2964−2969.
(70) Gupta, A., Reizman, I. M. B., Reisch, C. R., and Prather, K. L. J. (2017) Dynamic regulation of metabolic flux in engineered bacteria using a pathway-independent quorum-sensing circuit. *Nat. Biotechnol. 35* (3), 273−279.
(71) Dinh, C. V., and Prather, K. L. J. (2019) Development of an autonomous and bifunctional quorum-sensing circuit for metabolic flux control in engineered *Escherichia coli*. *Proc. Natl. Acad. Sci. U. S. A. 116* (51), 25562−25568.
(72) Nielsen, A. A. K., Der, B. S., Shin, J., Vaidyanathan, P., Paralanov, V., Strychalski, E. A., Ross, D., Densmore, D., and Voigt, C. A. (2016) Genetic circuit design automation. *Science 352* (6281), aac7341.
(73) Thompson, M. G., Pearson, A. N., Barajas, J. F., Cruz-Morales, P., Sedaghatian, N., Costello, Z., Garber, M. E., Incha, M. R., Valencia, L. E., Baidoo, E. E. K., Martin, H. G., Mukhopadhyay, A., and Keasling, J. D. (2020) Identification, characterization, and application of a highly sensitive lactam biosensor from *Pseudomonas putida*. *ACS Synth. Biol. 9* (1), 53−62.
(74) Chen, Y., Ho, J. M. L., Shis, D. L., Gupta, C., Long, J., Wagner, D. S., Ott, W., Josić, K., and Bennett, M. R. (2018) Tuning the dynamic range of bacterial promoters regulated by ligand-inducible transcription factors. *Nat. Commun. 9* (1), 64.
(75) Wu, Y. K., Chen, T. C., Liu, Y. F., Tian, R. Z., Lv, X. Q., Li, J. H., Du, G. C., Chen, J., Ledesma-Amaro, R., and Liu, L. (2020) Design of a programmable biosensor-CRISPRi genetic circuits for dynamic and autonomous dual-control of metabolic flux in *Bacillus subtilis*. *Nucleic Acids Res. 48* (2), 996−1009.
(76) Thompson, M. G., Sedaghatian, N., Barajas, J. F., Wehrs, M., Bailey, C. B., Kaplan, N., Hillson, N. J., Mukhopadhyay, A., and Keasling, J. D. (2018) Isolation and characterization of novel mutations in the pSC101 origin that increase copy number. *Sci. Rep. 8* (1), 1590.
(77) Siedler, S., Khatri, N. K., Zsohár, A., Kjærbølling, I., Vogt, M., Hammar, P., Nielsen, C. F., Marienhagen, J., Sommer, M. O. A., and Joensson, H. N. (2017) Development of a bacterial biosensor for rapid screening of yeast *p*-coumaric acid production. *ACS Synth. Biol. 6* (10), 1860−1869.

https://doi.org/10.1021/acssynbio.0c00252
ACS Synth. Biol. XXXX, XXX, XXX−XXX

(78) Hicks, M., Bachmann, T. T., and Wang, B. J. (2020) Synthetic biology enables programmable cell-based biosensors. *ChemPhysChem 21* (2), 132−144.
(79) Li, H., Liang, C. N., Chen, W., Jin, J. M., Tang, S. Y., and Tao, Y. (2017) Monitoring in vivo metabolic flux with a designed whole-cell metabolite biosensor of shikimic acid. *Biosens. Bioelectron. 98*, 457−465.
(80) Liang, C. N., Zhang, X. X., Wu, J. Y., Mu, S. S., Wu, Z., Jin, J. M., and Tang, S. Y. (2020) Dynamic control of toxic natural product biosynthesis by an artificial regulatory circuit. *Metab. Eng. 57*, 239−246.
(81) Collins, C. H., Leadbetter, J. R., and Arnold, F. H. (2006) Dual selection enhances the signaling specificity of a variant of the quorum-sensing transcriptional activator LuxR. *Nat. Biotechnol. 24* (6), 708−712.
(82) Faure, G., Ogurtsov, A. Y., Shabalina, S. A., and Koonin, E. V. (2016) Role of mRNA structure in the control of protein folding. *Nucleic Acids Res. 44* (22), 10898−10911.
(83) Carbonell, P., Radivojevic, T., and García Martín, H. G. (2019) Opportunities at the intersection of synthetic biology, machine learning, and automation. *ACS Synth. Biol. 8* (7), 1474−1477.
(84) Guo, J. H., Wang, T. M., Guan, C. G., Liu, B., Luo, C., Xie, Z., Zhang, C., and Xing, X. H. (2018) Improved sgRNA design in bacteria via genome-wide activity profiling. *Nucleic Acids Res. 46* (14), 7052−7069.
(85) Hanko, E. K. R., Paiva, A. C., Jonczyk, M., Abbott, M., Minton, N. P., and Malys, N. (2020) A genome-wide approach for identification and characterisation of metabolite-inducible systems. *Nat. Commun. 11* (1), 1213.
(86) Canton, B., Labno, A., and Endy, D. (2008) Refinement and standardization of synthetic biological parts and devices. *Nat. Biotechnol. 26* (7), 787−793.
(87) Gao, C., Hou, J. S., Xu, P., Guo, L., Chen, X. L., Hu, G. P., Ye, C., Edwards, H., Chen, J., Chen, W., and Liu, L. M. (2019) Programmable biomolecular switches for rewiring flux in *Escherichia coli*. *Nat. Commun. 10* (1), 3751.
(88) Dahl, R. H., Zhang, F. Z., Alonso-Gutierrez, J., Baidoo, E., Batth, T. S., Redding-Johanson, A. M., Petzold, C. J., Mukhopadhyay, A., Lee, T. S., Adams, P. D., and Keasling, J. D. (2013) Engineering dynamic pathway regulation using stress-response promoters. *Nat. Biotechnol. 31* (11), 1039−1046.
(89) Xu, P., Wang, W. Y., Li, L. Y., Bhan, N., Zhang, F. M., and Koffas, M. A. G. (2014) Design and kinetic analysis of a hybrid promoter−regulator system for malonyl-CoA sensing in *Escherichia coli*. *ACS Chem. Biol. 9* (2), 451−458.
(90) Riglar, D. T., Richmond, D. L., Potvin-Trottier, L., Verdegaal, A. A., Naydich, A. D., Bakshi, S., Leoncini, E., Lyon, L. G., Paulsson, J., and Silver, P. A. (2019) Bacterial variability in the mammalian gut captured by a single-cell synthetic oscillator. *Nat. Commun. 10* (1), 4665.
(91) Guiziou, S., Sauveplane, V., Chang, H. J., Clerté, C., Declerck, N., Jules, M., and Bonnet, J. (2016) A part toolbox to tune genetic expression in *Bacillus subtilis*. *Nucleic Acids Res. 44* (15), gkw624.
(92) Chen, K. M., Cofer, E. M., Zhou, J., and Troyanskaya, O. G. (2019) Selene: a PyTorch-based deep learning library for sequence data. *Nat. Methods 16* (4), 315−318.

https://doi.org/10.1021/acssynbio.0c00252
ACS Synth. Biol. XXXX, XXX, XXX−XXX